



EVALUATION OF ANTICANCER ACTIVITY OF PLANT MEDIATED IRON OXIDE NANOPARTICLES USING RHAZYA STRICTA

Muhammad Numan^{1*}, Mudassar Iqbal^{2*} and Hassan Wahab³

^{1*,2*}Department of Agricultural Chemistry & Biochemistry, The University of Agriculture Peshawar, Pakistan

³Physics Division, Pakistan Institute of Nuclear Science and Technology, Nilore, Islamabad Pakistan

*Corresponding authors: Muhammad Numan, Mudassar Iqbal

*E-mail: numan.dawezai@gmail.com, mudassariqbal@aup.edu.pk

Abstract

Green synthesis is an effective method for the synthesis of nanoparticles (NPs), so the objective of this project was to synthesis FeNPs using the crude extract from *Rhazya stricta*, a green synthesis approach. After the synthesis different microscopic as well spectroscopic techniques, including XRD, UV/VIS, SEM and EDX were used to confirm the synthesis as well as size and shape of the synthesized FeNPs. The resulting product was found to be 48.32 nm at 2 mM concentration. The synthesized nanoparticles were then tested for their cytotoxicity using Brine shrimps lethality test as *in-vitro* and human hepatocellular carcinoma cancer lines huH-1 as *in-vivo*. The brine shrimps lethality (BSL) assays showed concentration-dependent mortality where maximum (43.3%) mortality was observed at 100 $\mu\text{g. mL}^{-1}$ and minimum mortality (6.7%) at 5 $\mu\text{g. mL}^{-1}$ after 48 hrs. The IC₅₀ of the FeNPs against brine shrimps was observed as 137.4 μM while the standard Etoposide was 33.4 μM after 48 hrs. During the *in-vivo* cytotoxicity test against huH-1 has confined the non-toxicity behavior of the synthesized FeNPs, where at a maximum concentration (500 $\mu\text{g /ml}$) the FeNPs revealed 52.5% cell viability with 654.8 μM IC₅₀ values. It is clear from the result that the biosynthesized FeNPs using *R. stricta* possess less cytotoxic and are effectively safe. The *in vivo* cytotoxicity against huH-1 hepatoma cancer cell line also confined the non-toxicity of synthesized FeNPs where at a maximum concentration (500 $\mu\text{g /ml}$) the FeNPs revealed 52.5% cell viability with 654.8 μM IC₅₀ values. It is concluded that bio-mediated FeNPs were effective against cancer cell lines. Therefore, it is suggested that the bio-mediated NPs are safe and eco-friendly with no toxicity and could have overwhelming applications in health sciences.

Keywords: Plant-mediated nanoparticles, *Rhazya stricta*, Anticancer activity, brine shrimp lethality, Hepatocellular carcinoma

I. Introduction

Nanotechnology is primarily concerned with synthesizing, manipulating, and applying materials with dimensions ranging from less than a micron to distinct atoms. Through the development of NPs with a specific form, composition, size and other significant qualities, the scope of their uses in food, agriculture, textiles, medicine, cosmetics, and the environment has been assessed [1]. Metal nanoparticles such as Aluminum (Al), Titanium (Ti), Zinc (Zn), Palladium (Pd), Lead (Pb),

Cadmium (Cd), iron (Fe), Copper (Cu), Cobalt (Co), silver (Ag) and gold (Au) have increased much consideration in the current years because to their distinctive significance [2].

Nanotechnology is a multidisciplinary field with many applications in mechanics, electronics, catalysis, optics, magnetics, energy research, and biomedicine. Nanotechnology research and development spans many scientific disciplines, including material sciences, chemistry, physics, and biotechnology [3]. It is concerned with bi-functional macromolecules that can be used as tools to construct nano-objects as well as bio-fabrication of nano-objects. Later, microorganism compromises many benefits like wide-ranging physiological and genetic diversity for nanostructures synthesis and a key instrument for nanoscience [4]. The distinctive features of NPs such as improved solubility and multi-functionality, surface ability and high-volume surface ratio open novel potentials for biomedicine [5]. The electronic, electrical and optical properties of NPs are size reliant and numerous novel approaches for the size-controlled synthesis of AgNPs are being established [6].

The unique property of NPs is their size to the surface ratio making them more appropriate for application in catalysis, optoelectronics, pharmaceuticals, biological tagging and photonics [7]. Nanoparticles can be created via physical, chemical, biological, and hybrid approaches. However, chemical and physical techniques are also thriving and are considered to have pioneered the development of monodispersed nanoparticles. Besides nanotechnology, these methods are potentially hazardous, toxic and costly, energy requirement, high pressure and complex separation procedure. These approaches result in the presence of toxic chemicals adsorbed on the surface of nanoparticles, which may have a negative impact on biomedical techniques [8].

Nanotechnology has transformed various research fields and contributing a diverse group of applications in agriculture and biomedicine. Metallic nanoparticles, particularly iron oxide nanoparticles (FeNPs), have attained significant attention due to its small size with unique properties. However, traditional synthesis of NPs often involves hazardous chemicals and complex procedures, raising concerns regarding toxicity and environmental impact. In this perspective, the use of plant-mediated synthesis presents a novel and environmentally friendly approach. Evaluating the anticancer activity of plant-mediated synthesized FeNPs using *Rhazya stricta* show a novel contribution to the biomedical field, addressing the gap in research regarding eco-friendly nanoparticle synthesis and their application for cancer treatment. We hypothesized that plant-mediated FeNPs could reveal promising anticancer properties. Therefore, the present study was carried out to investigate the anticancer activity of *R. stricta* aqueous extract and *R. stricta*-mediated FeNPs and to explore its potential as a viable alternative in cancer therapy.

II. Materials and methods

2.1. Plant collection and extraction

Aerial parts of *Rhazya stricta* were collected from with the permission of local forest officer from district Karak, Khyber Pakhtunkhwa- Pakistan located at 33°7'12N 71°5'41E. The collection of plants was carried out in accordance with international guidelines to maintain the integrity of sample [9]. The plant sample in clean paper bag was transferred to laboratory within 48 hours, a specimen was deposited in herbarium at the University of Agriculture Peshawar Pakistan under voucher no MIK-6/22-021. The plant samples were cleaned with distilled water, dried at room temperature and grinded in an electric grinder. The extract was prepared by mixing 5 g of finely powdered material with 50 mL of deionized water. The mixture was heated to 60 °C under continuous stirring for 30 minutes. After cooling to room temperature, the resulting solution was filtered through Whatman filter paper No.1. The solution was subsequently centrifuged at 6000 rpm for 15 minutes at room temperature. The supernatant was carefully collected and stored in a freezer at 4 °C and used within 3-4 days (34).

2.2. Synthesis of Iron nanoparticle

Iron nanoparticles were synthesized by mixing 1 mM $\text{FeCl}_3 \cdot 6\text{H}_2\text{O}$ aqueous solution with 10 mL *R. stricta* aqueous leaf extract at room temperature. The color of the solution was changed which is an indicative of oxidation/reduction reaction. The cell filtrates (50 mL) was mixed with different concentrations of $\text{FeCl}_3 \cdot 6\text{H}_2\text{O}$ (1 mM, 2 mM, and 3 mM) at constant temperature (40°C). The mixture was centrifuged twice at 10000 rpm for 10 minutes. The flasks were placed on magnetic stirrer for 30 minutes. Variation in color after centrifugation and drying was observed and measured. To ensure the absence of trace aqueous extracts, Fe nanoparticles was re-dispersed in double distilled water and was allowed to dry in powder [10].

2.3. Sample Characterization:

The synthesized Fe_2O_3 NPs were exposed to various characterization methods to identify their specific properties. For optical properties, biosynthesized Fe nanoparticles was assessed using UV-Vis spectra (Optima SP3000+, Japan) within the wavelength ranging from 200 to 800 nm with a 1 nm band gap. Baseline correction of the spectrophotometer was carried out by using a blank reference and absorption spectra of all the samples were recorded. The UV-spectrum for all of the reactions were recorded at different concentration of $\text{FeCl}_3 \cdot \text{H}_2\text{O}$. SEM was used to determine the size and shape of Fe_2O_3 NPs. Using a Quanta Inspect F scan electron microscopy (SEM) operating at 25 kV in a vacuum. The prepared nanomaterial was mounted on aluminum subs having 25 diameters by using conductive sticky pads. The nanoparticle is coated with a fine layer of gold using a coating machine. To assess the shape and size of the synthesized nanoparticle, the sample was coated on SEM grid and examined under various magnifications. EDX (Energy dispersive X-ray) was used for the elemental composition of nanomaterial [11].

X-ray (XRD) diffraction technique was used to determine the crystal structure and grain size of biosynthesized Fe nanoparticles. The biosynthesized Fe nanoparticle using *R. stricta* (plant) were subjected to Powder X-ray diffraction PXRD (MODEL). The structural, elemental composition and particle size of the Fe_2O_3 NPs were characterized by using XRD. The XRD data was plotted using the origin software [12].

3.1. Bioassays of synthesized Iron nano particles

3.1.1. Brine-Shrimp Cytotoxicity

The cytotoxicity assay used brine shrimp larvae (*Artemia salina*) to determine the in vitro cytotoxicity potential of IONPs. *Artemia salina* eggs were incubated for 24-48 hours at 30 °C in 1 L of sterile sea saltwater in a glass jar with constant aeration. After the larvae hatched, active free floating nauplii were collected under light conditions and used for further investigation. Under light conditions, each nauplii was exposed to varying concentrations of iron NPs. The proportion of dead shrimps in each well was assessed after 48 hours of incubation, and the median lethal dose (IC₅₀) was computed using GraphPad software. [13]

The toxicity of biosynthesized iron nanoparticles was assessed using three doses (5, 25, 50, 75, and 100 $\text{g} \cdot \text{mL}^{-1}$) (Figure 1). The test samples were transferred to seawater with varying dose concentrations: 5, 25, 50, 75, and 1000 $\mu\text{g} \cdot \text{mL}^{-1}$ [14]. Thirty (30) shrimps were introduced to each vial and preserved for 48 hours; the remaining shrimps were counted.

$$\text{Mortality \%} = 100 - \left(\frac{\text{Shrimps in sample}}{\text{Total shrimps}} \right) \times 100$$

After the percent calculation, the inhibitory concentration dose (IC₅₀) was computed with the help of Prism graph pad software with 95% confidence intervals.

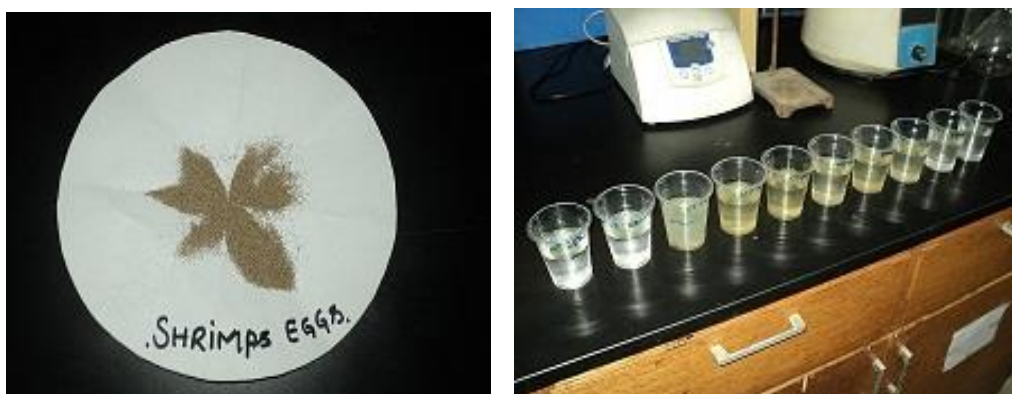


Figure 1. Cytotoxic effect of the biosynthesized FeNPs using *Rhazya stricta* at 1 mM tested against brine shrimps (Cytotoxic test).

3.1.2 Cytotoxicity Assay:

Cytotoxic effects of the newly biosynthesized synthesized iron oxide nanoparticles from *Rhazya stricta* and the same plant extract on huH-1 cells were determined using a crystal violet staining assay. Before the day of stimulation, 15000 cells per well were covered in 96- well plate. The next day cells were stimulated with serial dilution of nanoparticles and extract (500, 250, 100, 50, and 10 $\mu\text{g/ml}$). Then let the cells grow at 37 °C for 24 hrs. Media was removed after the accomplishment of stimulation time and cells were washed with PBS. For the crystal violet assay, 0.5 % crystal violet solution (50 μl per well) was added to stain the attached cells for 15 min at room temperature. To eliminate the remaining dye, the cells were gently rinsed and left for drying overnight. 50 μL of methanol per well was added and left on a bench rocker with a rate of 20 vibrations each minute and; incubate the plate with its cover for 20 minutes at room temperature. Using a plate reader, absorbance data was calculated at 550 nm (OD 550). A graph of viable cells against compounds concentration has been developed from the mean absorbance values by calculating the percentage growth of compounds treated cells against control cells [15].

3.2. Condition optimization for the induced biosynthesis of iron nanoparticles (FeNPs)

Condition optimization is an important factor that significantly influences the size distribution, type of biosynthesized iron nanoparticle and their stability. In the current research, the different condition was optimized for the induced biosynthesis of iron nanoparticles (FeNPs) by using an aqueous crude extract from *Rhazya Stricta* (Plant) as biological reducing agents. The Hexa-hydrated iron chloride ($\text{FeCl}_3 \cdot 6\text{H}_2\text{O}$) in different concentrations was used as a precursor for the synthesis of FeNPs at 40 °C. The aim of conducting experiments on different concentrations of $\text{FeCl}_3 \cdot 6\text{H}_2\text{O}$ was to activate the reduction of iron from its Fe^{+3} in $\text{FeCl}_3 \cdot 6\text{H}_2\text{O}$ to its free metallic form Fe^{+2} . The reduction of iron was initially observed using ultraviolet-visible (UV-Vis) spectroscopy [16].

IV. Results & Discussion

4.1 UV/Vis spectrophotometric analysis of FeNPs:

Iron nanoparticles (FeNPs) synthesis was confirmed by the characteristic change of *Rhazya stricta* extract and adding dropwise aqueous FeCl_3 into plant extract. The mixture color changed from yellowish-dark brown (Figure. 2). Color change indicates reduced Fe^{+3} into zero-valent iron form. The reduced Fe ions in aqueous solutions were observed by measuring UV-Vis spectra. The absorption spectra of green synthesized FeNPs were done at 200-450 nm wavelengths. Absorption peaks for FeNPs were observed at 200-250 nm ranges. The excitation of surface Plasmon, which is a coherent delocalized electron within any two material vibrations in FeNPs, has been testified previously [17]. The absorption peak around 236 nm (Figure 3) revealed that 2 mM concentration resulted in maximum nanoparticle synthesis. In size morphology and dissolution kinetics, the concentration of a medium plays an important role (Liu *et al.* 2001). In our research, the solution was adjusted at concentration 2 mM in 1:1 ratio of FeCl_3 and *Rhazya stricta* extract (Figure 3).

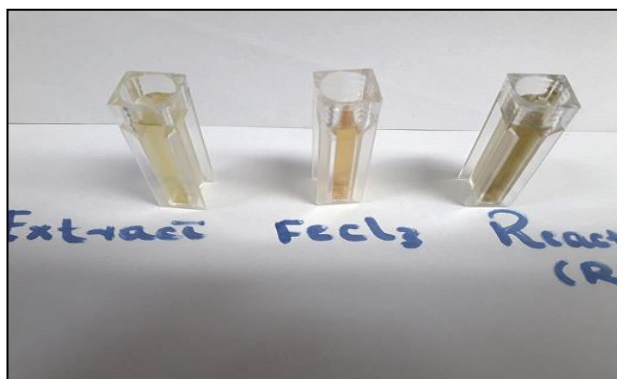


Figure 2. Photographs of pale yellow (plant extract), brown (FeCl_3), and dark brown (plant extract+ FeCl_3).

4.2 Effect of Precursor Salt Concentration on FeNPs Synthesis

Different concentrations (1, 2 and 3 mM) of precursor salt ($\text{FeCl}_3 \cdot 6\text{H}_2\text{O}$) to synthesize FeNPs under the same extract concentration from *Rhazya stricta*. The reaction mixture was allowed to complete for 30 minutes at 40°C . After 30 minutes, the UV-Vis absorption spectra were recorded for all three samples, which showed a promising change in the absorption value, indicating the effect of different concentrations in the reduction of iron from its Fe^{+3} in $\text{FeCl}_3 \cdot 6\text{H}_2\text{O}$ to its free metallic form Fe^{+2} as FeNPs. The surface plasmon absorption was observed at different values of the concentration. From the concentration of 1 mM of the precursor salt ($\text{FeCl}_3 \cdot 6\text{H}_2\text{O}$), the synthesized FeNPs gave a clear absorption peak at 242 nm, increased concentration of the precursor salt ($\text{FeCl}_3 \cdot 6\text{H}_2\text{O}$) an elevated absorption peak at 236 nm for 2 mM and 259 nm for 3 mM (Figure 3). Thus, it showed that concentration directly correlates with the absorption of UV-Vis light. Akhbari et al. (2019) [18] reported iron nanoparticle at wavelength of 216 and 284 nm. Ghosh et al., (2022) and Sandupatla et al., (2021) [19, 20] reported at 240 nm and 308nm peak of UV-Vis respectively.

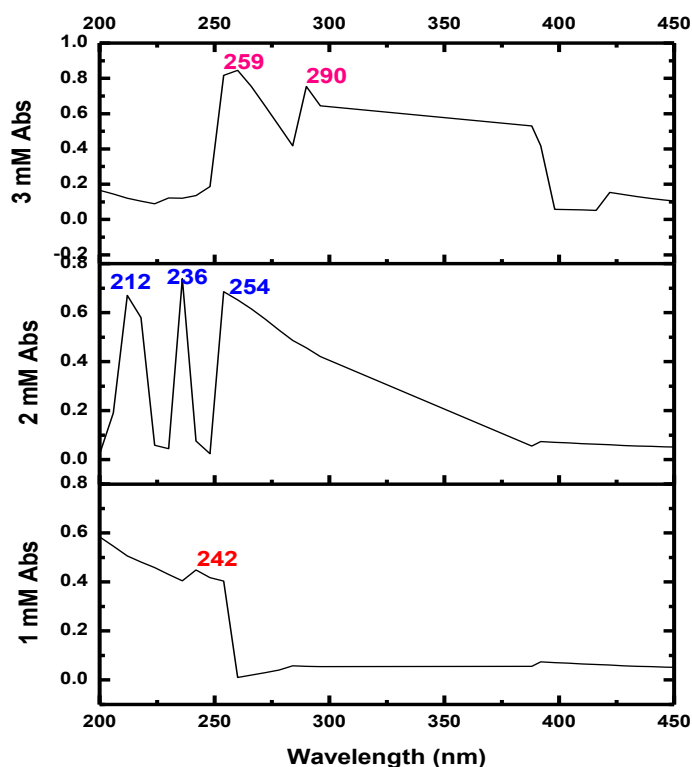


Figure 3 : UV-Visible spectra of biogenic Fe_2O_3 nanoparticles at concentration 1,2 and 3mM

4.3. Scan Electronic Microscope (SEM)

4.3.1 Effect of concentration of *R. stricta* on iron oxide nanoparticle size

The bio-synthesized FeNPs from different concentrations (1, 2 and 3 mM) at a constant temperature of 40 °C were subjected to a scanning electron microscope (SEM) to confirm their actual particle size, as shown in Figure 4. The SEM reveals the morphological features of biosynthesized FeNPs under the influence of the crude extract from *R. stricta* were conducted to test the role of molar ratio in forming iron oxide nanoparticles. From Figure 4 (b), it is quite clear that synthesized NPs at concentration 2 mM were spherical and symmetrical in shape, an aggregated molecule with an average size of 40nm and 50 nm. The aggregation and spherical shape are the indication of its magnetic features. The characterization results confirm the formation and presence of iron nanoparticles and biomolecules, which could help in capping the nanoparticles.

While at concentrations 1 mM and 3 mM, the particle size was considerably higher than 100 nm and was not the optimum condition for the synthesis of iron nanoparticles shown in Figure 4 (a) & (c). The SEM analysis reveals that *R. stricta* mediated iron nanoparticles at 1 mM were amorphous with a diameter greater than 100 nm.

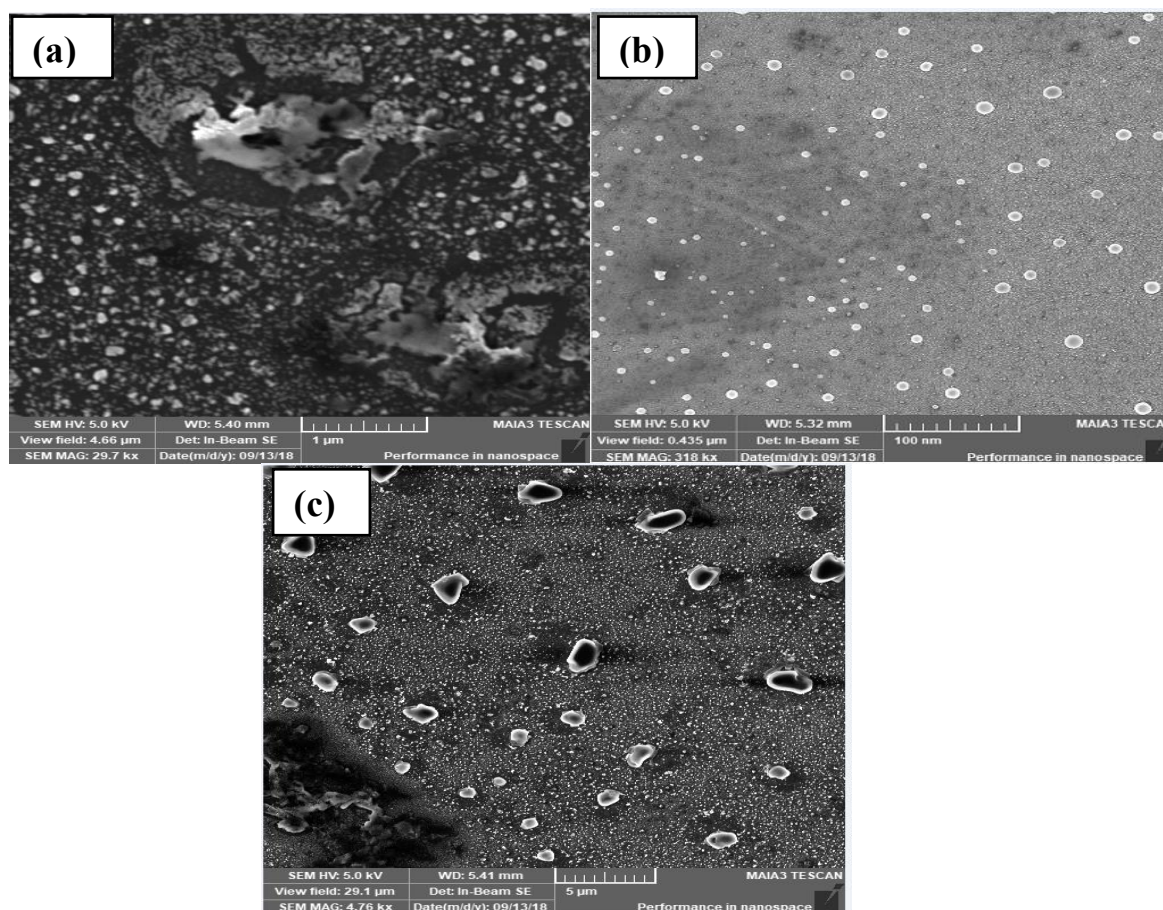


Figure 4. SEM micrographs of biosynthesized Iron nanoparticles synthesized using aqueous extracts of *R. stricta* at different concentrations 1 (a), 2(b), and 3 mM (c)

The biosynthesized iron nanoparticles EDX spectra from crude extracts of *R. stricta* give a clear indication regarding the elements of FeNPs. Figure 5 indicates a strong signal of iron atoms, confirming that FeNPs contain pure iron. Due to phytochemicals present in plant extracts of *R. stricta*, the elements of oxygen and carbon are contaminated around the peaks and these elements are the evidence of the organic substance attached to FeNPs. Chauhan and Upandhyay investigated *Lawsonia inermis* (Henna plant) mediated iron sulfate salt to FeNPs [21]. Various parameters such as salt concentration, temperature and pH were monitored and optimized for biosynthesis of iron nanoparticles. A concentration 0.02 molar of iron sulfate, pH 11 and a sample heated at 60 °C

temperature was found to be optimum for nanoparticle formation. Another experiment successfully prepared iron oxide nanoparticle using *Artemisia* leaves extract as a reducing agent. A cubical shape with an average range of 19-24 nm was obtained from SEM [22]. In this study, the concentration of salt and plant extract was 1:1. The results revealed a dependence on the particle size of FeNP and synthesis conditions.

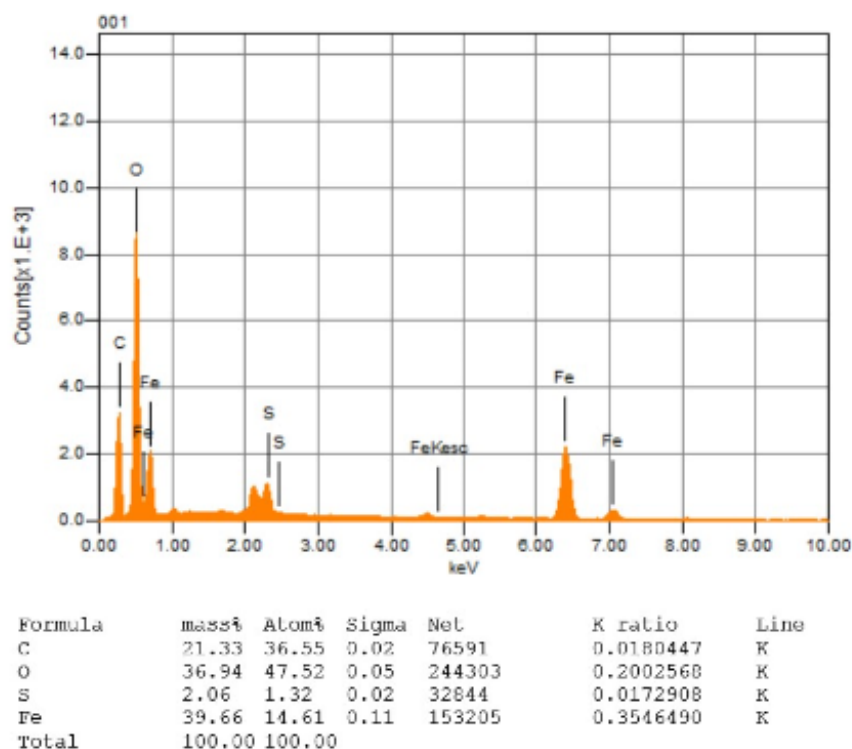


Figure 5. EDX of biosynthesized Iron nanoparticles synthesized using aqueous extracts of *R. stricta* at different concentrations 1 mM (a), 2 mM (b), and 3 mM (c).

4.4 XRD Diffraction of biosynthesized FeNPs using *R. stricta* at different concentration

The primary technique for determining the the crystalline structure and size of nanoparticles is X-ray diffraction (XRD), which was used to the biosynthesized iron nanoparticles (FeNPs) at different concentrations (1, 2, and 3 mM). The effective synthesis of FeNPs using *R. stricta* extract has been confirmed by the XRD patterns. Notably, as shown in Figure 6, the XRD analysis identified five unique distinctive peaks that aligned with the standard pattern.

The face-centered cubic (FCC) structure of the FeNPs obtained at 1 mM was shown in Figure 6(a), where five peaks were found at 2θ values of 30.20° , 35.62° , 43.29° , 57.3° , and 62.88° , corresponding to the (220), (311), (400), (511), and (440) planes of iron oxide. Based on the Scherrer equation, the average crystalline size was found to be 133.09 nm (Table 1).

Parallel to this, Figure 6(b) illustrates how FeNPs synthesised at 2 mM showed five peaks at 2θ values of 30.20° , 35.62° , 43.29° , 57.3° , and 62.88° , which correspond to the (220), (311), (400), (511), and (440) planes of iron oxide. Using the Scherrer equation, the average crystalline size was determined to be 48.32 nm (Table 1). FeNPs synthesized at 3 mM also exhibited five peaks at 2θ values of 30.20° , 35.62° , 43.29° , 57.3° , and 62.88° , corresponding to the (220), (311), (400), (511), and (440) planes of iron oxide, as depicted in Figure 18 (c). The average crystalline size was determined to be 177.06 nm using the Scherrer equation (Table 1). The XRD analysis from Figure 6 indicated that the sharpness of peaks differed among the concentrations, suggesting variations in nanoparticle sizes. Furthermore, the diffraction peaks of each concentration closely matched those of pure iron oxide, affirming the successful synthesis of FeNPs.

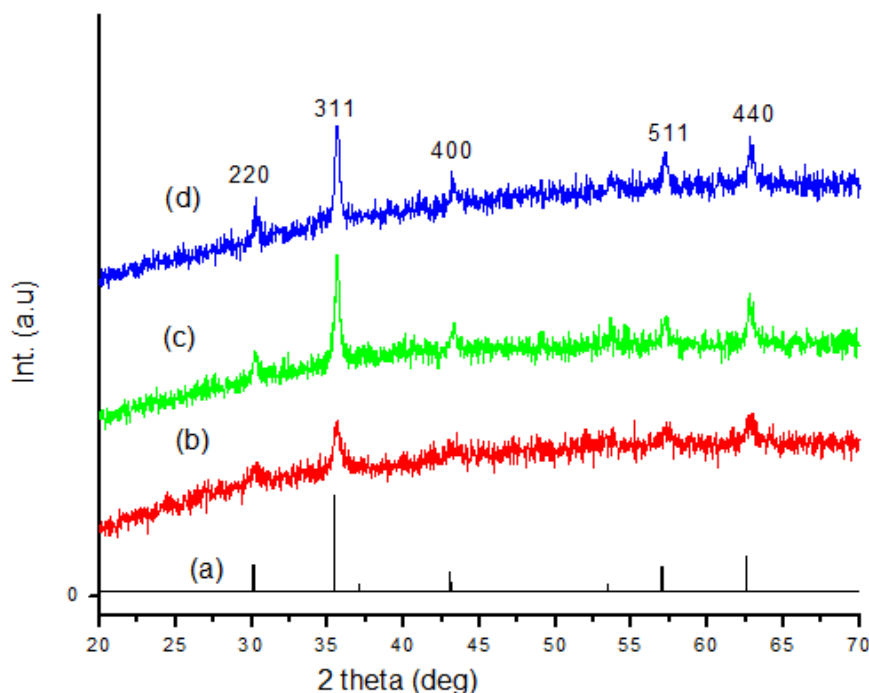


Figure 6. X-ray diffraction patterns for (a) pure iron oxide and for biosynthesized FeNPs fabricated from the reaction mixture of $\text{FeCl}_3 \cdot 6\text{H}_2\text{O}$ salt solution and *Rhazya stricta* prepared at different concentrations 1mM (a), 2mM (b) and 3 mM (c) respectively.

The size and morphology of nanoparticles could change by changing the concentration of metal precursor in a solution. The study conducted by Dubeya (2010) [35] on metal ion concentration for nanoparticle synthesis. The increasing trend of nanoparticles was observed by changing the metal ion concentration from 0.1 to 5 mM. Similar research was also conducted by Ahmad et al., (2016) on the concentration of gold NPs synthesis [35]. As the concentration of gold Au (III) from 1 mM to 5 mM increases, the production of gold nanoparticles increases.

Table 1. Particle size calculation at different concentrations of *Rhazya stricta* through X-pert high score.

Concentration (mM)	Peak	(hkl)	Peak position(2θ)	FWHM	Average Particle size(nm)
1	1	(220)	30.2	0.1	133.09
	2	(311)	35.62	0.409	
	3	(400)	43.29	0.201	
	4	(511)	57.3	0.05	
	5	440	62.88	0.03	
2	1	(220)	30.2	0.509	48.32
	2	(311)	35.62	0.509	
	3	(400)	43.29	0.102	
	4	(511)	57.3	0.401	
	5	440	62.88	0.101	
3	1	(220)	30.2	0.03	177.06
	2	(311)	35.62	0.05	
	3	(400)	43.29	0.03	
	4	(511)	57.3	0.309	
	5	440	62.88	0.101	

4.5 IC₅₀ values calculation

Rhazya stricta and biosynthesized iron nanoparticles in different concentrations IC₅₀ or IC₂₀ values were calculated using a Hill function through nonlinear regression analysis. The IC₅₀ values were transformed into log values for the assay comparisons using Linear Regression analysis.

4.6 Brine shrimps lethality (BSL)

The biosynthesized iron nanoparticles prepared from *Rhazya stricta* at 1 mM concentration with an average size 50 nm were screened against *Artemia salina* (brine-shrimp eggs) to measure the mortality/lethality. Brine shrimps (*Artemia salina*) are unicellular organisms that could be used as a standard to screen the cytotoxic effect of iron nanoparticles. The present study aims to evaluate the cytotoxic effect of FeNPs against brine shrimps. Different concentrations (5, 25, 50, 75 and 100 µg. mL⁻¹) of the prepared biosynthesized iron nanoparticles were performed in triplicates and compared with the control and standard drug Etoposide. The mortality in percent was calculated after 48 hrs. The maximum mortality (43.3%) at 100 µg. mL⁻¹ and minimum mortality (6.7%) at 5 µg. mL⁻¹ was observed after 48 hrs. While in standard etoposide at 100 µg. mL⁻¹ concentration, the highest mortality rate (90%) was observed after 48 hrs (Table 5). Moreover, biosynthesized FeNPs size (48nm) has highest mortality of brine shrimp as compared to FeNPs size (77nm). IC₅₀ of the FeNPs against brine shrimps were observed as (137.4 µM) after 48hrs by using Prism graph pad package. While, the IC₅₀ of the standard positive drug, Etoposide is 33.4 µM. From IC₅₀ of Etoposide it is clear that biosynthesized FeNPs using *Rhazya stricta* possesses less cytotoxic and is effectively safe (Figure 6).

Table 5. Percent mortality of biosynthesized FeNPS using *R. stricta* against brine shrimp after 48hrs.

Dose (µg/ml)		No of Shrimps	No of survivors	% Mortality	
Biogenic FeNPs	48 nm	5	30	28.0±0.61 ab	6.7±0.96 h
		25	30	25.0±0.58 cd	16.1±1.47 g
		50	30	21.0±0.58 e	30.0±0.62 de
		75	30	19.0±0.55 f	36.7±0.96 c
		100	30	27.0±0.58 ab	43.3±1.30 b
	77 nm	5	30	28.3±0.67 a	7.2±2.42 h
		25	30	26.3±0.33 bc	13.3±0.96 g
		50	30	23.7±0.88 d	22.8±1.47 f
		75	30	21.7±0.33 e	29.4±1.47 e
		100	30	20.0±0.58 ef	33.9±0.56 cd
Standard (Etoposide)		30	3.0±0.58 g	90.7±2.33 a	
LSD (<i>P</i> <0.05)		-	1.71	4.23	

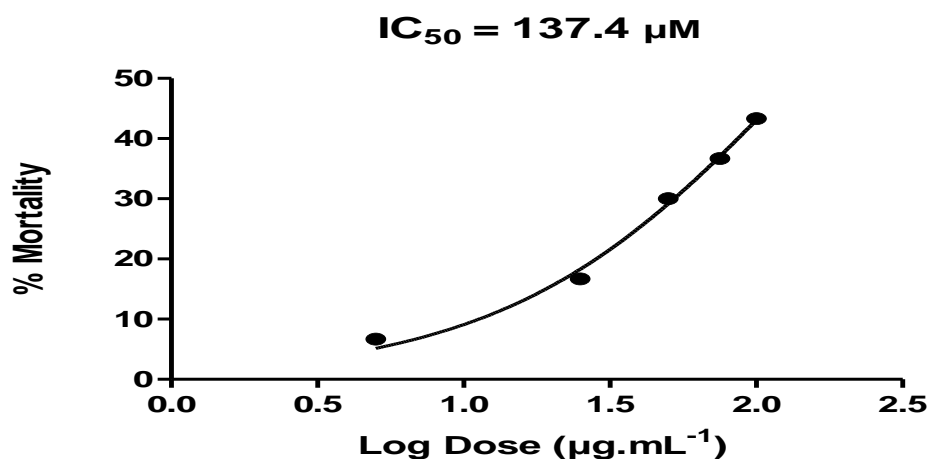


Figure 6. IC₅₀ value calculation of iron nanoparticles using Prism graph pad software.

FeNPs were successfully synthesized using a green approach from *Rhazya stricta* (plant) in the present study, which showed less cytotoxic effects used in different concentrations. Hence these iron nanoparticles prepared from *Rhazya stricta* are effective and safe when used at optimal concentrations. The future scope of the study would focus on determining the various applications of biosynthesized iron nanoparticles synthesized can be utilized in agriculture and medical fields.

Nanoparticle synthesis via physical and chemical methods results in good nanoparticles with defined size and shape, but the overall process is costly and produces toxic by-product substances that contribute to environmental problems. Therefore, nanoparticle synthesized by such approaches nullifies the scope in an area like medicine, health and drug delivery [24]. This has led to the growing interest of researchers in the “Greener Approach,” which results in the production of environmentally friendly NPs and prevents the release of toxic compounds into the atmosphere during or after the process [25].

The nanoparticle is an emerging technology used in commercially available products and still the risk factor of nano-substances is not known. For this purpose, the toxicity of nanomaterial determination is necessary. Many scientists have focused on brine shrimp (*Artemia salina*) lethality test in drug discovery to the toxic effect of various nanomaterials [26]. Similarly, Izadiyan et al. [27] synthesized IONPs from *Juglans regia*. The synthesized NPs have a non-toxic effect on normal and cancerous cervical cell lines. The FeNPs did not show any cytotoxicity to the brine shrimp. The eco-friendly synthesis of FeNPs from dried ginger has proved convenient and inexpensive and can be safely used in a wide range of medical and dental fields [28].

4.7 Cytotoxicity Assay on human cancer cell lines

Human cancer cell lines huH-1 were exposed to biologically synthesized iron oxide nanoparticles via *Rhazya stricta* plant at concentrations of 500, 250, 100, 50 and 10 ng for 24 h and cytotoxicity was determined using MTT assays. All the tests are carried out in triplicate. Untreated cells were used as a positive control. We calculated the percentages viability of huH-1 cell lines by treating them with different concentrations (0-100) of produced iron nanoparticles via biological method from *Rhazya stricta* and then made a comparison between the percentages of cell viabilities biogenic iron nanoparticles and aqueous plant extract (*R. stricta*).

With increasing concentration of biologically synthesized nanoparticles, the viability decreases, and the same is the case with plant extract *R. stricta* and cytotoxicity was observed in a dose-dependent fashion. However, the cytotoxicity of biologically synthesized iron oxide nanoparticles is more than the cytotoxicity of using only plant extract.

Moreover, the biogenic FeNPs size (48 nm) exhibited a maximum cell death rate, resulting in minimum % viability than biogenic FeNPs size (77 nm) and plant extract. This indicates that a smaller NPs size has a greater surface area and the highest efficacy against huH-1 cancer cell lines and consequently has the highest cell death rate and lowest cell viability. Moreover, large-size NPs (77 nm) has a lower surface area, which is less efficient against huH-1 cancer cell lines.

Nonetheless, at lower concentrations of biologically synthesized NPs and plant extract has the lowest cell death rate. The biosynthesized FeNPs and aqueous extract of *R. stricta* showed potent cytotoxicity against hepatoma human (huH-1) cancer cell lines in a dose-

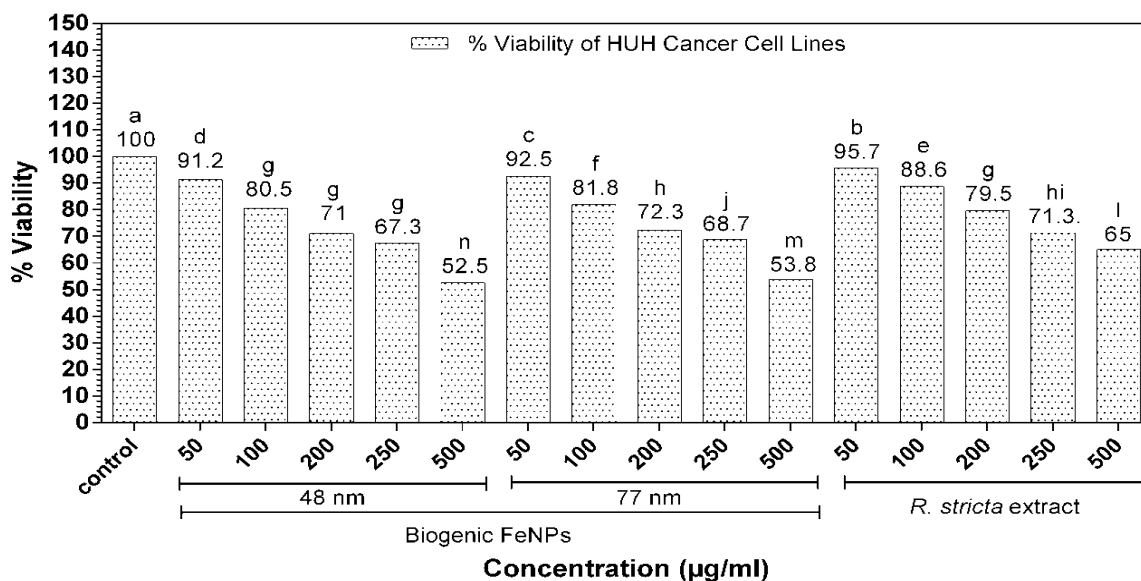


Figure 7. Percent (%) viability of biogenic synthesized iron nanoparticle and *R. stricta* on liver cancer cell lines (huH-1 cell lines at different concentrations).

dependent manner. Apparently, the percent viability decreased by increasing the concentration of both FeNPs and aqueous plant extract (Figure 7). However, at a maximum concentration (500 µg/ml), the iron nanoparticle revealed 52.5% cell viability as compared to the extract of *R. stricta*, in which 65% cells were viable at 500 µg/ml concentration. At a minimum concentration 50 µg/ml, the biosynthesized iron nanoparticle displayed 91.2% of the cell were viable, while at the same concentration, the aqueous extract of *R. stricta* revealed 95.7% cell viability.

In the cytotoxicity activity of iron nanoparticles and *R. stricta* extract against hepatoma cancer cell lines, the IC₅₀ value was also determined by using prism graph pad 4.5 software. The IC₅₀ value for *R. stricta* and biosynthesized iron nanoparticles was 654.8 µM and 116.7 µM, respectively. The lower value of IC₅₀ for FeNPs indicates that biologically synthesized FeNPs have a more potent cytotoxic effect on human cancer cell lines than an aqueous plant extract.

Our results demonstrate that *R. stricta* aqueous extract and iron nanoparticles reasonably affect hepatic carcinoma cells. It has been reported that crude extracts of *R. stricta* induce apoptosis in human cancer cell lines [29]. Iron nanoparticles being in nanometers, can easily penetrate the cytoplasm and nuclear membrane and damage the DNA, which may produce ROS. These high ROS can break hydrogen bonds in DNA molecules, decreasing cell proliferation [30]. Nanoparticles are considered viable options in the treatment of cancer. Shosha et al. [31] characterized iron nanoparticles by various techniques. The iron nanoparticle was evaluated to inspect their cytotoxic effect against K562 (human leukemia), THLE2 (human normal epithelial liver), SNU-182 and (human hepatocellular carcinoma) and revealed cytotoxic effects against these. Another study conducted by Yang et al. [32] on amine-modified iron nanoparticles and reported 25 % reduction in human dermal fibroblast at 224 µg/mL concentration. In a similar study, Namvar et al. [33] biosynthesized FeNPs from seaweed (*Sargassum muticum*) aqueous extract and assessed their IC₅₀ value against Hep G2, MCF-7, HeLa and Jurkat cell lines were 23.83 µg/mL, 18.75 µg/mL 12.5 µg/mL and 6.4 µg/mL respectively 72 hours after treatment.

V. Conclusion

The domains of biotechnology, nanotechnology, and medicine all make extensive use of IONPs. Researchers have been focusing on developing fast and economical processes for synthesizing IONPs in recent years. *R. stricta* aqueous extract was used to produce IONPs in this study, which used green synthesis. Brine shrimps' lethality (BSL) assays show maximum mortality (43.3%) at 100 µg. mL⁻¹ after 48 Hrs as compared to plant extract. Cytotoxicity assay shows that increasing the

concentration of biological FeNPs decreases the viability of huH-1 cancer cell line. Moreover, biogenic FeNPs and *R. stricta* extract has IC₅₀ values 654.8 μ M and 116.7 μ M, respectively. This study will be useful for future scientists interested in exploring the fields of nanobiotechnology and nanomedicine, since it will provide a foundation for researchers studying nanocarrier systems and drug delivery metabolisms. Therefore, it is suggested that the bio-mediated NPs are safe, eco-friendly with no toxicity and could have overwhelming applications in agriculture and biomedical sciences.

Author Contributions: Conceptualization, M.N and M.I, methodology, M.N.; software, M.N; validation, M.I; formal analysis, M.I and M.N; investigation, M.I; resources, M.I; data curation, M.I.; writing original draft preparation, M.N; writing review and editing, M.N and M.I; visualization, M.N.; supervision, M.I; project administration, M.I; funding acquisition, M.I and M.N.

Acknowledgments:

This article is based on the PhD thesis research of Mr. Muhammad Numan. We gratefully acknowledge Dr. Hassan Wahab Chief Scientist Pakistan Institute of Nuclear Science and Technology (PINSTECH) for their technical support in research activities.

Conflicts of Interest: The authors declare no conflict of interest.

References

1. Oza, G., S. Pandey, A. Gupta, R. Kesarkar and M. Sharon. 2012. Biosynthetic reduction of gold ions to gold nanoparticles by *Nocardia farcinica*. *J. Microbiol. Biotechnol. Res.* 2: 511–515.
2. Nasreen, I., T. C. Hulkoti and P. Taranath. 2014. Biosynthesis of nanoparticles using microbes. *A Review, Collids and surface B. Bioinformatics.* 121: 474-483.
3. Rai, M., Birla, S., Ingle, A. P., Gupta, I., Gade, A., Abd-Elsalam, K., ... & Duran, N. (2014). Nanosilver: an inorganic nanoparticle with myriad potential applications. *Nanotechnology Reviews*, 3(3), 281-309.
4. Villaverde, A. 2010. Nanotechnology, Bionanotechnology and Microbial Cell Factories. *J. Microb. Cell. Biol.* 9: 53-60.
5. Gao, J and B. Xu. 2009. Applications of Nanomaterials inside Cells. *J. Nano. Technol.* 4: 37–51.
6. Li, Y., N. Y. Kim, E. J. Lee, W. P. Cai and S. O. Cho. 2006. Synthesis of Silver Nanoparticles by Electron Irradiation of Silver Acetate. *Nucl. Instrum. Methods.* 251: 425–428.
7. Venkatesan, B., V. Subramanian, Tumala and A. Vellaichamy. 2014. Rapid synthesis of biocompatible silver nanoparticles using aqueous extract of *Rosa damascena* petals and evaluation of their anticancer activity. *Asian. Pac. J. Trop. Med.* 7: 294-300.
8. Jain, D., S. Kachhwaha, R. Jain, G. Srivastava and S. L. Kothari. 2010. Novel Microbial Route to Synthesize Silver Nanoparticles Using Spore Crystal Mixture of *Bacillus thuringiensis*. *Ind. J. Experi. Biol.* 48: 1152-115.
9. World Health Organization. (2003). WHO guidelines on good agricultural and collection practices [GACP] for medicinal plants. World Health Organization.
10. Storozhuk, L., Besenhard, M. O., Mourdikoudis, S., LaGrow, A. P., Lees, M. R., Tung, L. D., Gavriilidis, A., Thanh, N.T.K. and Thanh, N. T. K. (2021). Stable iron oxide nanoflowers with exceptional magnetic heating efficiency: simple and fast polyol synthesis. *ACS Applied Materials & Interfaces*, 13(38): 45870-45880.
11. Mishra, R. K., A. K. Zachariah and S. Thomas. 2017. Energy-dispersive X-ray spectroscopy techniques for nanomaterial. In *Microscopy Methods in Nanomaterials Characterization* (pp. 383-405). Elsevier.

12. Shukla, A., Singha, R. K., Sasaki, T., Prasad, V. V., & Bal, R. (2019). Synthesis of Highly Active Pd Nanoparticles Supported Iron Oxide Catalyst for Selective Hydrogenation and Cross-Coupling Reactions in Aqueous Medium. *Chemistry Select*, 4(17): 5019-5032.
13. Ishwarya, R., Tamilmani, G., Al-Ghanim, K. A., Govindarajan, M., Nicoletti, M., & Vaseeharan, B. (2023). Biosynthesis of zinc oxide nanoparticles from molted feathers of *Pavo cristatus* and their antibiofilm and anticancer activities. *Green Processing and Synthesis*, 12(1), 20230090.
14. Khalil, A. T., Ovais, M., Ullah, I., Ali, M., Shinwari, Z. K., & Maaza, M. (2017). Biosynthesis of iron oxide (Fe₂O₃) nanoparticles via aqueous extracts of *Sageretia thea* (Osbeck.) and their pharmacognostic properties. *Green Chemistry Letters and Reviews*, 10(4), 186-201.
15. Albeshri, A., N.A. Baeshen, T.A. Bouback and A.A. Aljaddawi. 2021. A Review of *Rhazya stricta* Decne Phytochemistry, Bioactivities, Pharmacological Activities, Toxicity, and Folkloric Medicinal Uses. *Plants*. 10(11): 2508.
16. Yassin, M. T., Al-Otibi, F. O., Al-Askar, A. A., & Alharbi, R. I. (2023). Green synthesis, characterization, and antifungal efficiency of biogenic iron oxide nanoparticles. *Applied Sciences*, 13(17), 9942.
17. Samarawickrama, K.G.R., U.G.S. Wijayapala and C.A.N. Fernando. 2022. Green Synthesis of Iron Nanoparticles from Long coriander (*Eryngium foetidum*) Leaves Aqueous Extract.
18. Akhbari, M., Hajiaghaee, R., Ghafar zadegan, R., Hamedi, S., & Yaghoobi, M. (2019). Process optimisation for green synthesis of zero-valent iron nanoparticles using *Mentha piperita*. *IET nanobiotechnology*, 13(2), 160-169.
19. Ghosh, S., Bloch, K., & Webster, T. J. (2022). Bioprospecting of novel algal species with nanobiotechnology. In *An Integration of Phycoremediation Processes in Wastewater Treatment* (pp. 41-74). Elsevier.
20. Sandupatla, R., Dongamanti, A., & Koyyati, R. (2021). Antimicrobial and antioxidant activities of phytosynthesized Ag, Fe and bimetallic Fe-Ag nanoparticles using *Passiflora edulis*: A comparative study. *Materials Today: Proceedings*, 44, 2665-2673.
21. Chauhan, S. and Upadhyay, L.S.B. 2019. Biosynthesis of iron oxide nanoparticles using plant derivatives of *Lawsonia inermis* (Henna) and its surface modification for biomedical application. *Nanotechnology for Environmental Engineering*, 4(1): 1-10.
22. Bouafia, A., S.E. Laouini, A. Khelef, M.L. Tedjani and F. Guemari. 2021. Effect of ferric chloride concentration on the type of magnetite (Fe₃O₄) nanoparticles biosynthesized by aqueous leaves extract of artemisia and assessment of their antioxidant activities. *Journal of Cluster Science*, 32(4): 1033-1041.
23. Vitta, Y., M. Figueroa, M. Calderon and C. Ciangherotti. 2020. Synthesis of iron nanoparticles from aqueous extract of *Eucalyptus robusta* Sm and evaluation of antioxidant and antimicrobial activity. *Materials science for energy technologies*, 3, 97-103.
24. Parashar, U. K., P. S. Saxena and A. Srivastava. 2009a. Bioinspired synthesis of silver nanoparticles. *Digest. J. Nanomat. Biostruc. (DJNB)*. 4(1).
25. Rani, M., Yadav, J., Chaudhary, S., & Shanker, U. (2021). An updated review on synthetic approaches of green nanomaterials and their application for removal of water pollutants: Current challenges, assessment and future perspectives. *Journal of Environmental Chemical Engineering*, 9(6), 106763.
26. Muhammad, W., Ullah, N., Khan, M., Ahmad, W., Khan, M. Q., & Abbasi, B. H. (2019). Why Brine shrimp (*Artemia salina*) larvae is used as system for nanomaterials? The science of procedure and nano-toxicology: a review. *Int. J. Biosci*, 14(5), 156-176.
27. Izadiyan, Z., K. Shameli, M. Miyake, H. Hara, S.E.B. Mohamad, K. Kalantari, S.H. Taib and E. Rasouli. 2020. Cytotoxicity assay of plant-mediated synthesized iron oxide nanoparticles using *Juglans regia* green husk extract. *Arabian Journal of Chemistry*. 13(1): 2011-2023.
28. Akifa, B., M. Jeevitha, S. Preetha and S. Rajeshkumar. 2020. Cytotoxicity of Iron Nanoparticles Synthesized Using Dried Ginger. *J. Pharma. Res. Int.* 32(25): 112-118.

29. El-Ghazali, G.E., K.S. Al-Khalifa, G.A. Saleem and E.M. Abdallah. 2010. Traditional medicinal plants indigenous to Al-Rass province, Saudi Arabia. *J. Med. Plants Res.* 4(24): 2680-2683.
30. Sudharshan, S. J and M. Dyavaiah. 2021. Astaxanthin protects oxidative stress mediated DNA damage and enhances longevity in *Saccharomyces cerevisiae*. *Biogerontology*, 22(1): 81-100.
31. Shosha, N. N. H., S. Elmasry, M. Moawad, S. H. Ismail and M. Elsayed. 2022. In vivo and in vitro evaluation of antitumor effects of iron oxide and folate core shell-iron oxide nanoparticles. *Brazilian J. Biol.* 84.
32. Yang, W., J. Lee, S. Hong, J. Lee and D. W. Han. 2013. Difference between toxicities of iron oxide magnetic nanoparticles with various surface-functional groups against human normal fibroblasts and fibrosarcoma cells. *Materials*. 6: 4689-4706.
33. Namvar, F., H. S. Rahman, R. Mohamad, J. Baharara, M. Mahdavi, E. Amini, M.S. Chartrand and S.K. Yeap. 2014. Cytotoxic effect of magnetic iron oxide nanoparticles synthesized via seaweed aqueous extract. *Int. J. Nanomed.* 9: 2479-2488.
34. Al-Sahli, S. A., Al-Otibi, F., Alharbi, R. I., Amina, M., & Al Musayeib, N. M. (2024). Silver nanoparticles improve the fungicidal properties of *Rhazya stricta* decne aqueous extract against plant pathogens. *Scientific Reports*, 14(1), 1297.
35. Dubey, S. P., Lahtinen, M., & Sillanpää, M. (2010). Tansy fruit mediated greener synthesis of silver and gold nanoparticles. *Process Biochemistry*, 45(7), 1065-1071.
36. Ahmad, N., Ricolleau, C., bouar, Y. L., & Alloyeau, D. (2016, November). Shape transformations during the growth of gold nanostructures. In *European Microscopy Congress 2016: Proceedings* (pp. 161-162). Weinheim, Germany: Wiley-VCH Verlag GmbH & Co. KGaA.